FSMI: Fast computation of Shannon Mutual Information for information-theoretic mapping

Zhengdong Zhang, Trevor Henderson, Vivienne Sze, Sertac Karaman

Abstract— **Information-based mapping algorithms are critical to robot exploration tasks in several applications ranging from disaster response to space exploration. Unfortunately, most existing information-based mapping algorithms are plagued by the computational difficulty of evaluating the Shannon mutual information between potential future sensor measurements and the map. This has lead researchers to develop approximate methods, such as Cauchy-Schwarz Quadratic Mutual Information (CSQMI). In this paper, we propose a new algorithm, called Fast Shannon Mutual Information (FSMI), which is significantly faster than existing methods at computing the *exact* Shannon mutual information. The key insight behind FSMI is recognizing that the integral over the sensor beam can be evaluated analytically, removing an expensive numerical integration. In addition, we provide a number of approximation techniques for FSMI, which significantly improve computation time. Equipped with these approximation techniques, the FSMI algorithm is more than three orders of magnitude faster than the existing computation for Shannon mutual information; it also outperforms the CSQMI algorithm significantly, being roughly twice as fast, in our experiments.**

I. Introduction

Robot exploration tasks are embedded and essential in several applications of robotics, including disaster response and space exploration. The key to efficient robot exploration is to identify and navigate to locations that will yield the most information towards building a map of the environment.

The problem of robotic exploration has received a large amount of attention over the past few decades, resulting in a rich literature. The *geometry-based frontier exploration algorithms* approach this problem with heuristics that typically navigate the robot to the frontier of the well known portion of the environment [1]–[5]. These heuristics are very efficient from a computational point of view. However, they lack any rigorous reasoning about information, which makes them relatively inefficient in terms of the path spanned by the robot while the exploring the environment [6]–[11].

On the other hand, *information-based mapping and exploration* techniques consider paths that aim to maximize principled information-theoretic metrics to actively maximize the information collected by the robot. While information-based mapping algorithms using Shannon mutual information (MI) provide guarantees on the exploration of the environment, the evaluation of Shannon MI, *e.g.*, in [12], is computational demanding. The run time of the algorithm scales quadratically with the spatial resolution of the occupancy grid and linearly with the numerical integration resolution due to the absence of an analytical solution. It has been pointed out that the speed at which mutual information is evaluated can limit the planning frequency, which in turn limits the velocity of the robot and the exploration speed of the environment [13]. Towards designing algorithms that are computationally more efficient, Charrow et al. [14] proposed the use of an alternative information metric, called Cauchy-Schwarz Quadratic Mutual Information (CSQMI). They show that the integrations in CSQMI can be computed analytically. Additionally, they show a close approximation of CSQMI can be evaluated in time that scales linearly with respect to the spatial resolution of the occupancy grid. It is reported in [14] that CSQMI can be computed substantially faster than Shannon MI, and it behaves similarly to Shannon MI in experiments. Several follow-up publications on information-theoretic autonomous mapping systems adopt CSQMI as the information metric [13], [15], [16].

In this paper, we propose a new algorithm, called Fast Shannon Mutual Information (FSMI), that computes the (Shannon) MI in an efficient manner. We recognize that the main computational bottleneck in the MI computation reported by Julian et al. [12] is that the MI between a beam and a single cell requires a computationally-demanding numerical integration. The key idea behind the FSMI algorithm is to evaluate the MI between a measurement and all occupancy-grid cells that it intersects together. The shared computation between multiple cells is rearranged to give the integration an analytic form. As a result, FSMI's asymptotic run time is independent of the integration operation.

In addition, we adopt the approximation technique introduced for CSQMI in [14] to the FSMI algorithm, which renders an algorithm with a runtime that scales linearly with the spatial resolution, with negligible loss in accuracy. We show that, even though this approximate FSMI algorithm has the same asymptotic computational complexity when compared to the approximate CSQMI algorithm, an implementation of the approximate FSMI algorithm requires less than half the number of multiplications as an equivalent implementation of CSQMI, which translates to $1.8\times$ speed in our experiments. Finally, we show that, if the measurement noise is uniformly distributed, the Shannon MI can be evaluated exactly in linear time with respect to occupancy-grid resolution.

This paper is organized as follows. Section II introduces our notation and preliminary definitions. Section III presents the FSMI algorithm, proves its guarantees on correctness and computational complexity. Sections IV and V present two variants of FSMI with better run time. Finally, Section VI demonstrates the effectiveness of the FSMI algorithm in both synthetic and real experiments.

The authors are with the Massachusetts Institute of Technology.

II. Notation and Preliminary Definitions

A. The Occupancy-grid Map

We use the occupancy-grid map method to model the environment. As is standard, we assume that all the occupancy cells are independent and that a Bayesian filter is used to update the occupancy probabilities. The occupancy grid is denoted by the random variables $M = \{M_1, \ldots, M_K\}$, where K is the number of cells and $M_i \in \{0, 1\}$ is the binary random variable that indicates the occupancy of i-th cell. In this case, $M_i = 0$ indicates an empty cell, $M_i = 1$ indicates an occupied cell. The realization of the the random variable M_i is denoted by m_i. The robot is equipped with a range measurement sensor.

The depth measurement is denoted by the random variable Z, with realizations denoted by z. The measurement obtained at time t is denoted by z_t, and the set of measurements obtained up to time t is denoted by $z_{1:t}$. Typically, the robot acquires multiple measurements at the same time, *e.g.*, measuring range in different directions. Then, all range measurements are denoted by $z_t = (z_t^1, \ldots, z_t^{n_z})$, where n_z is the number of beams in a scan. Unless explicitly stated otherwise, we assume that the noise distribution follows a zero mean Gaussian with a constant standard deviation of σ.The measurements obtained by the robot are a stochastic function of the map, the sensor model, and the state of the robot. The state of the robot is described by the variable x. In this paper, the state variables encode the pose of the robot. We denote the state at time t by x_t. We denote the sequence of states from the initial time through time t by $x_{1:t}$.

The standard independence assumption among the occupancy cells is assumed, *i.e.*, $P(M_1 = m_1, \ldots, M_K = m_k | z_{1:t}, x_{1:t}) = \prod_{1 \le i \le K} P(M_i = m_i | z_{1:t}, x_{1:t})$ where $P(\cdot)$ is the probability function. In addition, we assume no prior information on the occupancy grid cell, meaning that $P(M_i = 1) = P(M_i = 0) = 0.5$. Hence, the standard Bayesian filter can be used to update the occupancy map based on the scanning results:

$$\begin{aligned}\frac{P(M_i = 1 | z_{1:t}, x_{1:t})}{P(M_i = 0 | z_{1:t}, x_{1:t})} = &\frac{P(M_i = 1 | z_{1:(t-1)}, x_{1:(t-1)})}{P(M_i = 0 | z_{1:(t-1)}, x_{1:(t-1)})} \\ &\frac{P(M_i = 1 | z_t, x_t)}{P(M_i = 0 | z_t, x_t)}.\end{aligned} \tag{1}$$

We denote the probability of occupancy of the ith cell by $o_i = P(M_i = 1 | z_{1:t}, x_{1:t})$. Additionally, we denote the odds ratio of a cell $r_i = o_i/(1 - o_i)$. The Bayesian filter in Equation (1) essentially updates r_i for the cells according to the acquired range measurements.

B. Shannon Mutual Information Metric

In this section, we review the algorithm proposed by [12] that computes the Shannon mutual information for a single range measurement. For notational convenience, we omit the conditional probability terms $x_{1:t}$ and $z_{1:t}$. With a slight abuse of notation, we use $M = (M_1, ..., M_n)$ to represent the cells that a single sensor range measurement (beam) intersects. We further assume that cells in M are listed in an ascending order by their distance from the sensor. Again by a slight abuse of notation, We denote the measurement of this single beam by Z. In addition, let $\delta_i(z)$ approximate the odds ratio inverse sensing model [17] for the cell M_i:

$$\delta_i(z) = \begin{cases} \delta_{occ} & z \text{ indicates } M_i \text{ is occupied} \\ \delta_{emp} & z \text{ indicates } M_i \text{ is empty} \\ 1 & \text{otherwise} \end{cases},$$

where $\delta_{occ} > 1$ and $\delta_{emp} < 1$ are hyper parameters. Then,

$$I(M_i; Z) = \int_{z \ge 0} P(Z = z) f(\delta_i(z), r_i) dz, \tag{2}$$

where $P(Z = z)$ is the measurement prior and

$$f(\delta, r) = \log\left(\frac{r + 1}{r + \delta^{-1}}\right) - \frac{\log \delta}{r\delta + 1}.$$

Since Eq. (2) does not have a known analytical solution, [12] evaluate it numerically by discretizing z:

$$I(M_i; Z) = \sum_z P(Z = z) f(\delta_i(z), r_i) \lambda_z^{-1},$$

where λ_z is the discretization resolution. The mutual information for the whole beam is computed as the sum of each $I(M_i; Z)$. Hence, the computational complexity is $O(n^2 \lambda_z)$.

C. Cauchy-Schwarz Quadratic Mutual Information Metric

The Cauchy-Schwarz quadratic mutual information (CSQMI) is an alternative metric of Shannon mutual information. It was shown in [14] that the CSQMI metric for a sensor beam that intersects with n cells can be evaluated analytically in $O(n^2)$ time. This is lower than the $O(n^2 \lambda_z)$ complexity of Shannon mutual information, because numerical integration is avoided. We reiterate the formula to compute CSQMI [14]:

$$\begin{aligned} I_{CS}(M; Z) = &\log \sum_{l=0}^{C} w_l \mathcal{N}(0, 2\sigma^2) + \log\Big(\prod_{i=1}^{n} (o_i^2 + (1 - o_i)^2) \\ &\sum_{j=0}^{n} \sum_{l=0}^{n} P(e_j) P(e_l) \mathcal{N}(\mu_l - \mu_j, 2\sigma^2)\Big) \\ &- 2 \log \sum_{j=0}^{n} \sum_{l=0}^{n} P(e_j) w_l \mathcal{N}(\mu_l - \mu_j, 2\sigma^2), \end{aligned} \tag{3}$$

where $\mathcal{N}(x, \sigma^2)$ is the probability density function at x of a normal distribution of zero mean and standard derivation of σ, μ_l is the distance from the center of the l-th cell to the depth sensor and $w_l = P(e_l)^2 \prod_{j<l} (o_j^2 + (1 - o_j)^2)$.

Authors in [14] also proposed a close approximation to CSQMI that truncates the tails of a Gaussian distribution to zero. This enables CSQMI to be computed approximately in $O(n)$, as each double sum in Eq. (3) can be approximated:

$$\sum_{j=0}^{n} \sum_{l=j-\Delta}^{j+\Delta} \alpha_{j,l} \mathcal{N}(\mu_l - \mu_j, 2\sigma^2),$$

where $\alpha_{j,l}$ represents the corresponding coefficient in the double sum, and Δ is a small constant such as 3.

D. Problem Formulation

A typical information-theoretic exploration strategy is to generate a set of potential trajectories, evaluate mutual information along each of trajectory, and choose the one with the highest mutual information per travel cost [13]–[16].

In order to evaluate the mutual information along a trajectory, the trajectory is typically discretized in the state space, the mutual information is computed at each state and then

summed. Hence, the fundamental problem of information-based exploration using range sensing is to efficiently evaluate the mutual information between the map and one range measurement. This problem is solved many times in mutual-information-based exploration algorithms. We call this the *single-beam mutual-information computation* problem.

Consider a sensor that emits a single beam for depth measurement. Let $M' = (M_1, \ldots, M_n)$ be a vector of binary random variables representing all the occupancy cells that the sensor beam can intersect. Let the random variable Z be a potential future depth measurement. We wish to measure the mutual dependence between these random variables using Shannon mutual information. The mutual information between the beam and a single cell can be computed using Eq. (2). As is standard, we decompose the mutual information between the beam and all of the cells in M', *i.e.*, $I(M'; Z)$, into the following summation:

$$\begin{aligned} &\sum_{i=1}^{n} I(M_i; Z) = \sum_{i=1}^{n} \int_{z \geq 0} P(Z = z) f(\delta_i(z), r_i) dz \\ &= \sum_{i=1}^{n} \int_{z \geq 0} P(Z = z) \Big(\log \left(\frac{r+1}{r + \delta^{-1}} \right) - \frac{\log \delta}{r\delta + 1} \Big) dz, \end{aligned} \tag{4}$$

where $P(Z = z)$ is the measurement prior. This paper focuses on efficient algorithms and efficient approximations for computing the quantity defined in Eqn. (4).

III. The Fast Shannon Mutual Information (FSMI) Algorithm for 2D Mapping

This section is devoted to the presentation of the FSMI algorithm.

A. The FSMI Algorithm

In this section we present the Fast Shannon Mutual Information (FSMI) algorithm. The key idea behind the FSMI algorithm is the following: Instead of performing the summation in Eq. (4) directly, FSMI computes $I(M'; Z)$ holistically and analytically evaluates one of the resulting integrals, which leads to substantial computational savings.

Algorithm 1 summarizes this procedure with subroutines in Algorithms 2 and 3. To describe the algorithms, let us first present our notation. Let l_i be the distance from the origin to the ith cell where $l_1 = 0$ and l_i is monotonically increasing. See the top part of Figure 1. Let us denote the center of the ith cell by $\mu_i = (l_i + l_{i+1})/2$. Same as [12], we use $P(e_j)$ to denote the probability that the jth cell is the first non-empty cell in M', *i.e.*, $P(e_j) = o_j \prod_{i<j} (1 - o_i)$. Let $P(e_0)$ be the probability that all cells are empty. $\Phi(\cdot)$ denotes the standard normal CDF. We also define $C_k = f(\delta_{occ}, r_k) + \sum_{i<k} f(\delta_{emp}, r_i)$ and $G_{j,k} = \int_{l_k}^{l_{k+1}} P(z|e_j) dz$.

B. Correctness of the FSMI algorithm

The following theorem states the correctness of the FSMI algorithm, that is, the FSMI algorithm indeed returns the Shannon mutual information $I(M; Z)$.

Theorem 1 (Correctness of FSMI): The Shannon mutual information between the depth measurement and all of the cells in M is $I(M'; Z) = \sum_{j=0}^{n} \sum_{k=1}^{n} P(e_j) C_k G_{k,j}$.

Algorithm 1 The FSMI algorithm

Require: σ and l_i, o_i for $1 \leq i \leq n$.
1: $I \leftarrow 0$
2: Compute $P(e_j)$ for $0 \leq j \leq n$ with Algorithm 2.
3: Compute C_k for $1 \leq k \leq n$ with Algorithm 3.
4: **for** $j = 0$ **to** n **do**
5: **for** $k = 0$ **to** n **do**
6: $G_{k,j} \leftarrow \Phi((l_{k+1} - \mu_j)/\sigma_j) - \Phi((l_k - \mu_j)/\sigma_j)$
7: $I \leftarrow I + P(e_j) C_k G_{k,j}$
8: **return** I

Algorithm 2 Evaluate $P(e_j)$ for $0 \leq j \leq n$

Require: o_i for $1 \leq i \leq n$
1: $E_0 \leftarrow 1$
2: **for** $j = 1$ **to** n **do**
3: $E_j \leftarrow E_{j-1}(1 - o_j)$
4: $P(e_j) \leftarrow E_{j-1} o_j$
5: $P(e_0) = E_n$
6: **return** $P(e_j)$ for $0 \leq j \leq n$

Algorithm 3 Evaluate C_k for $1 \leq k \leq n$

Require: $\delta_{emp}, \delta_{occ}$ and r_i for $1 \leq i \leq n$
1: $q_0 = 0$
2: **for** $k = 1$ **to** n **do**
3: $q_k = q_{k-1} + f(\delta_{emp}, r_k)$
4: $C_k = q_{k-1} + f(\delta_{occ}, r_k)$
5: **return** C_k for $1 \leq k \leq n$

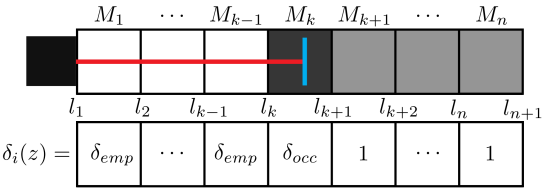

Fig. 1. Illustration of the key idea behind the proof of Lemma 1. The sensor beam (red) hits an obstacle (blue) in cell M_k. The value of the odds ratio inverse sensor model is shown below.

We first prove the following intermediate result regarding the structure of $f(\delta, r)$. Let $F(z) = \sum_{i=1}^{n} f(\delta_i(z), r_i)$.

Lemma 1 (Piecewise Constant Summation): The function $F(z) = \sum_{i=1}^{n} f(\delta_i(z), r_i)$ is piecewise constant. In particular, if z lies in the k-th cell, *i.e.*, $l_k \leq z < l_{k+1}$, then $F(z) = C_k$ where $C_k = f(\delta_{occ}, r_k) + \sum_{i<k} f(\delta_{emp}, r_i)$.

Proof: For $i < k$ a measurement of z implies that the beam has passed through M_i. Therefore M_i should be empty and $\delta_i(z) = \delta_{emp}$. By definition, $\delta_k(z) = \delta_{occ}$. A measurement of z also indicates that the beam stops at cell k which gives no information about cells M_j for $j > k$, so $f(\delta_j(z), r_j) = f(1, r_j) = 0$. Therefore each term of $F(z)$ is constant for $l_k \leq z \leq l_k + 1$ and the sum is equal to the desired C_k, proving the lemma. ■

Lemma 1 shows that the function $F(z)$ change its value

only at the cell boundaries, as z increases. (See Fig. 1 for an illustration.) If we compute at once the mutual information between a range measurement and *all* the cells it can intersect, we can turn the integration in Eq. (2) into a sum.

Proof: (Theorem 1) We begin with the total Shannon mutual information for one range measurement as stated in Eq. (4). We substitute the definition of Shannon mutual information provided in Eq. (2), and rearrange to reveal the sum described in Lemma 1. We find that $I(M';Z)$ equals

$$\begin{aligned}
&\sum_{i=1}^{n} I(M_i;Z) = \sum_{i=1}^{n} \int_z P(z) f(\delta_i(z), r) dz \\
&= \sum_{i=1}^{n} \int_z \sum_{j=0}^{n} P(e_j) P(z|e_j) f(\delta_i(z), r) dz \\
&= \sum_{j=0}^{n} P(e_j) \int_z P(z|e_j) \left(\sum_{i=1}^{n} f(\delta_i(z), r_i) \right) dz \\
&= \sum_{j=0}^{n} P(e_j) \int_z P(z|e_j) F(z) dz.
\end{aligned} \tag{5}$$

Inspired by the result of Lemma 1, we divide the integration over z into a sum of multiple integration intervals across each cell boundary. This allows us to isolate the described term that is constant across each cell as follows:

$$\begin{aligned}
I(M';Z) &= \sum_{j=0}^{n} P(e_j) \sum_{k=1}^{n} \int_{l_k}^{l_{k+1}} P(z|e_j) C_k dz \\
&= \sum_{j=0}^{n} \sum_{k=1}^{n} P(e_j) C_k \int_{l_k}^{l_{k+1}} P(z|e_j) dz \\
&= \sum_{j=0}^{n} \sum_{k=1}^{n} P(e_j) C_k G_{k,j}.
\end{aligned}$$

This completes the proof. ∎

C. Computational Complexity of the FSMI Algorithm

We study the time complexity of Algorithm 1 with respect to, n, the number of cells that a single range measurement intersects. The result is stated in the following theorem:

Theorem 2: Algorithm 1 has $O(n^2)$ time complexity.

The proof of Theorem 2 is straightforward with the following intermediate results:

Lemma 2: $P(e_j)$ can be computed for all of $0 \leq j \leq n$ in $O(n)$ with Algorithm 2.

Lemma 3: C_k can be computed for for all of $1 \leq k \leq n$ in $O(n)$ with Algorithm 3.

Lemma 4: The standard normal CDF, $\Phi(\cdot)$, can be evaluated with a look-up table. $G_{k,j}$ can be evaluated in $O(1)$ as follows: $G_{k,j} = \Phi\left((l_{k+1} - \mu_j)/\sigma\right) - \Phi\left((l_k - \mu_j)/\sigma\right)$.

Note that, unlike the algorithm proposed in [12], the FSMI algorithm does not perform any numerical integration. As a result the complexity of FSMI outperforms the algorithm in [12] by a factor of λ_z, the integration resolution.

Remark 1: FSMI has the same time complexity as the exact version of CSQMI.

Since we assume the noise distribution has constant σ, we can directly precompute $\Phi(\frac{\cdot}{\sigma})$ to avoid one division operation per query. Note that in addition to tabulating $\Phi(\cdot)$, we also build look-up table for $f(\delta_{occ}, r_i)$ and $f(\delta_{emp}, r_i)$ for all i, which can be computationally expensive if we use their definition to evaluate them. Specifically, We precompute $f(\delta_{occ}, r_i)$ and $f(\delta_{emp}, r_i)$ for a discrete set of values of r_i and store the results in a look-up table. We set $\delta_{emp}\delta_{occ} = 1$, following [12]; Since $f(\delta_{emp}, r_i) = f(\delta_{occ}, 1/r_i)$, a single look-up table suffices.

IV. Efficient Implementations via Gaussian Truncation

In [14], the authors approximate the CSQMI metric by setting the tail of the Gaussian noise distribution to zero. We apply their technique to FSMI. Let Δ be the truncation width. We approximate the equation in Theorem 1 as

$$I(M';Z) = \sum_{j=0}^{n} \sum_{k=j-\Delta}^{j+\Delta} P(e_j) C_k G_{k,j}. \tag{6}$$

We refer to the variation of FSMI that applies the approximation described above as *Approx-FSMI*. We refer to the corresponding CSQMI algorithm with the same approximation as the *Approx-CSQMI*. The complexity of evaluating Approx-FSMI is $O(n\Delta)$, same as Approx-CSQMI in [14].

Even though both algorithms have the same asymptotic complexity, we argue that the Approx-FSMI algorithm can be implemented so that it requires fewer multiplications when compared to the Approx-CSQMI algorithm. Intuitively, this is because our computation in Eq. (6) has only one double summation while the approximate version of CSQMI in Eq. (3) has two similarly structured double summations of the same size. In this comparison, we omit other operations, *e.g.*, additions, because they are significantly cheaper than multiplications on both general purpose CPUs and FPGAs [18]. Operations such as $\log(\cdot)$ occur at very low frequency in both Eq. (6) and Eq. (3).

Theorem 3 (Number of Multiplications): Evaluating Approx-FSMI and Approx-CSQMI require $(\Delta + 3)n$ and $(2\Delta + 9)n$ multiplications, respectively.

V. Shannon Mutual Information Under Uniform Measurement Noise Model (Uniform FSMI)

Recall that the asymptotic time complexity of Approx-FSMI is $O(n\Delta)$. In this section, we show that when the sensor noise follows a uniform distribution, under reasonable technical assumptions, the Shannon mutual information can be evaluated in $O(n)$, independently of Δ.

Theorem 4 (Uniform FSMI): Suppose that cells have constant width, *i.e.*, for all i, $l_{i+1} - l_i = \Delta L$. Suppose that the sensor noise model is uniform and that the limits are quantized onto cell boundaries:

$$P(Z|e_i) \sim U[l_i - H\Delta L,\ l_{i+1} + H\Delta L], \tag{7}$$

for $H \in \mathbb{Z}^+$. Let $D_i = \sum_{j \leq i} C_j$ for $1 \leq i \leq n$ and $D_i = 0$ otherwise. Then the Shannon mutual information between the beam and all the cells it intersects is

$$I(M';Z) = \sum_{j=0}^{n} P(e_j) \frac{D_{j+H} - D_{j-H-1}}{2H+1}$$

Proof: This proof follows the proof of Theorem 1 until Eq. (5). We plug in the PDF of the uniform distribution:

$$I(M';Z) = \sum_{j=0}^{n}\sum_{k=1}^{n} P(e_j)C_k \int_{l_k}^{l_{k+1}} P(z|e_j)dz$$

$$= \sum_{j=0}^{n} P(e_j) \sum_{k=j-H}^{j+H} \frac{C_k}{2H+1} = \sum_{j=0}^{n} P(e_j) \frac{D_{j+H} - D_{j-H-1}}{2H+1}$$

This completes the proof. ■

The algorithm to compute uniform-FSMI is summarized in Algorithm 4. Its time complexity is $O(n)$, outperforming Approx-FSMI and Approx-CSQMI by a factor of Δ.

Algorithm 4 The Uniform-FSMI algorithm

Require: H and r_i, l_i for $1 \leq i \leq n$.

1: $I \leftarrow 0$
2: Compute $P(e_j)$ for $0 \leq j \leq n$ with Algorithm 2.
3: Compute C_k for $1 \leq k \leq n$ with Algorithm 3.
4: $D_k \leftarrow 0$
5: **for** $k = 1$ **to** n **do**
6: $\quad D_k \leftarrow D_{k-1} + C_k$
7: **for** $j = 0$ **to** n **do**
8: $\quad I \leftarrow I + P(e_j) \frac{D_{\min(n,j+H)} - D_{\max(0,j-H-1)}}{2H+1}$
9: **return** I

VI. Experimental Results

A. Computational Experiments for a Single Measurement

First we study the accuracy and throughput of evaluating the Shannon mutual information of a single beam. The length of the beam is $10\,\mathrm{m}$ and the resolution of the occupancy grid is $0.1\,\mathrm{m}$. The occupancy values are generated at random. We set $\delta_{occ} = 1/\delta_{emp} = 1.5$. The sensor noise model is a normal distribution with $\sigma = 0.05\,\mathrm{m}$ regardless of the travel distance of the beam. The speed of the algorithms is evaluated on a single core of an Intel Xeon E5-2695 CPU.

a) Comparison of Original MI, FSMI, and Approx-FSMI: We compare the average relative error and running time for the following algorithms in 10^4 trials: the original MI algorithm [12] with $\lambda_z = 0.01\,\mathrm{m}$, FSMI, and Approx-FSMI with $\Delta = 3$. The ground truth MI is obtained using the original MI algorithm [12] with a substantially better resolution of $\lambda_z = 10\,\mu\mathrm{m}$. The results are summarized in Fig. 2(a) and Fig. 2(b). We observe that the FSMI computes the MI more accurately than the original MI algorithm, despite running more than three orders of magnitude faster. The run time of Approx-FSMI is an additional 7 times faster than FSMI, and yet it is still more accurate when compared to the original algorithm with $\lambda_z = 0.01\,\mathrm{m}$. Notice that the relative error of Approx-FSMI is below 10^{-5}.

b) Comparison of Approx-FSMI, Approx-CSQMI, and Uniform FSMI: We use the same $\Delta = 3$ to cut the tails of the Gaussian distributions in Approx-FSMI and Approx-CSQMI. The results are shown in Fig. 2(c). It can be seen that Approx-FSMI is $1.7\times$ faster than Approx-CSQMI, and Uniform FSMI is $3\times$ faster than Approx-CSQMI. Note that the acceleration is not as great as the predicted acceleration in Theorem 3 because of compiler optimizations.

B. Simulations for Planar Mapping with a Ground Robot

This section presents results of a computational experiment in which a simulated ground robot explores a synthetic planar (2D) environment. The environment is $18\,\mathrm{m} \times 18\,\mathrm{m}$ and represented by an occupancy grid with resolution $0.1\,\mathrm{m}$. The robot is equipped with a 360° lidar with 180 beams. The maximum distance of the sensor is set to $5\,\mathrm{m}$ and the noise is Gaussian with $\sigma = 0.05\,\mathrm{m}$. We test four algorithms: Approx-FSMI with $\Delta = 3$, Approx-CSQMI with $\Delta = 3$, Uniform FSMI and a nearest frontier exploration method. For the first three information-theoretic mapping methods, the robot travels to the scanning location that maximizes the ratio between MI gain and the travel distance, which is computed using Dijkstra's algorithm [19]. For the nearest frontier exploration method, we implement the same algorithm used in the experiments of [14], in which the robot clusters the frontiers cells and travels to the closest cluster. The exploration terminates when the entropy of the map drops below a predefined threshold. For each algorithm, we perform three independent trials.

Fig. 3(a) shows the mapped environment, together with the exploration trajectory of one of the trials with Approx-FSMI in our simulations. Fig. 3(b) compares the length of the trajectory for each method, averaged over three trials. All three information theoretic mapping algorithms yield trajectories of similar length; these trajectories are roughly 16% shorter than the trajectories generated by the nearest frontier algorithm.

We also report the average speed of MI evaluation during the synthetic experiments. The results are consistent with the one beam synthetic experiment: Approx-CSQMI takes $12.4\,\mu\mathrm{s}$ per beam, Approx-FSMI takes $8.3\,\mu\mathrm{s}$ per beam, and Uniform FSMI takes $4.9\,\mu\mathrm{s}$ per beam. These times are smaller in this experiment because the beam length is $5m$ rather than $10m$ as in the previous experiment.

C. Planar Mapping Task involving a Ground Robot

Finally, we study the real-world performance of the MI computation on a 1/10th scale car with the goal of exploring a small ($< 8\,\mathrm{m} \times 8\,\mathrm{m}$) planar environment. The car is equipped with a Hokoyo UST-10LX lidar which has a 270° field of view and a range of $10\,\mathrm{m}$. In our experiments, the field of view and the range are limited to 230° and $3\,\mathrm{m}$,

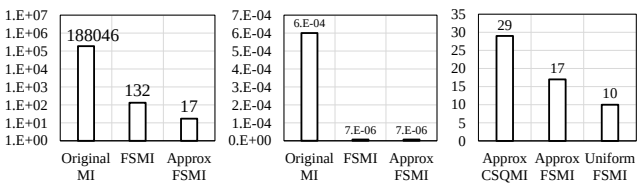

(a) Mean time (µs) (b) Mean relative error (c) Mean time (µs)

Fig. 2. Speed & relative error of different MI algorithms on a single beam.

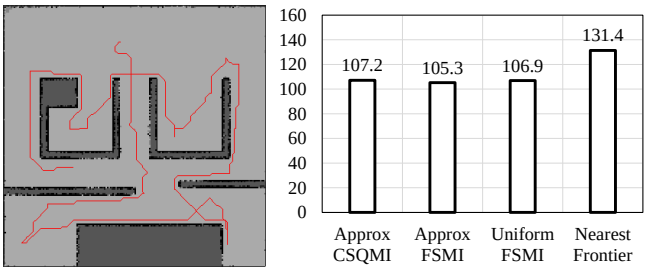

(a) Map and trajectory (b) Trajectory length

Fig. 3. Synthetic 2D environment exploration experiment results.

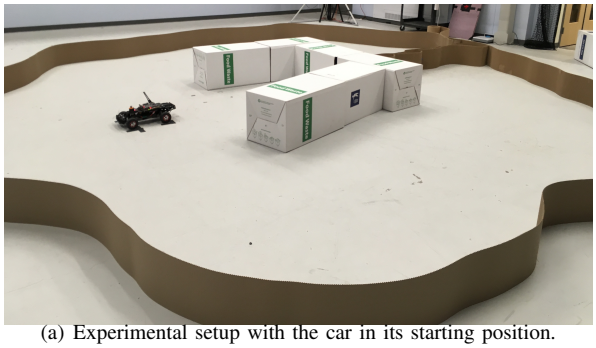

(a) Experimental setup with the car in its starting position.

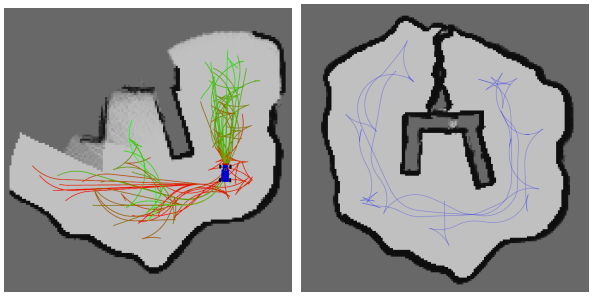

(b) RRT* based planner. Paths with high MI per meter are green.

(c) Complete map and trajectory for a trial with Approx-FSMI.

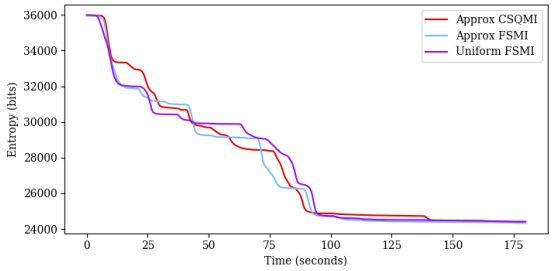

(d) Representative samples of the map's entropy during exploration

Fig. 4. Real experiments with a car in a 2D environment.

respectively. The number of measurements that fall within this field of view is 920. We assume perfect localization for this experiment. We use a motion capture system determine the pose of the car and send it to the car wirelessly. All other computational processing (MI computation, mapping, planning, control) is done on board with an Nvidia Jetson TX2 embedded ARM computer. Fig. 4(a) shows the setup of the experiment.

In order to plan feasible paths within the environment under the vehicle's dynamic constraint we use an RRT* motion planner [20] with Reeds-Shepp curves [21] as the steering function. After the number of nodes in the tree reaches a given limit, we evaluate the MI along each path in the tree at $0.2\,\mathrm{m}$ intervals, taking into account the independence between multiple beams according to [14]. To speed up computation, we only evaluate the MI for 50 beams per scanning location uniformly distributed in the field of view without noticeable loss of quality. The path with the highest total MI over travel distance is selected. A tree of possible paths and the corresponding score of each is shown in Fig. 4(b). The car then follows the selected path until it reaches the end at which point it replans. We terminate each experiment after 3 minutes which was sufficient for all trials. A completed map is show in Fig. 4(c).

Our experiments evaluate the performance of the following metrics: Approx-CSQMI with $\Delta = 3$, Approx-FSMI with $\Delta = 3$ and Uniform FSMI. For each metric, we performed four explorations from the same starting location and recorded the average time spent computing MI per sensor location along the path including the time spent performing independence checks (note that this time includes multiple beams). In all trials the resolution of the occupancy grid is $0.05\,\mathrm{m}$, $\sigma = 0.05\,\mathrm{m}$ and $\delta_{occ} = 1/\delta_{emp} = 1.5$. We measure Approx-CSQMI to take $422.7\,\mu\mathrm{s}$, Approx-FSMI to take $148.7\,\mu\mathrm{s}$ and Uniform FSMI to take $111.4\,\mu\mathrm{s}$ per sensor measurement. These results are consistent with, and in fact outperform the synthetic results which may be due to differences in the ARM architecture. Because the environment is small and the car is moving slowly the difference between methods is not evident in the overall exploration time as shown in Fig. 4(d).

VII. Conclusion

In this paper, we introduced the Fast Shannon Mutual Information (FSMI) algorithm for computing the Shannon mutual information between potential future measurements and the occupancy grid. We also introduced two variants. The Approx-FSMI approximates FSMI with arbitrary precision. The Uniform-FSMI algorithm computes the exact Shannon mutual information under the assumption that the measurement noise is uniformly distributed. We have proved guarantees on the correctness and the computational complexity of the proposed algorithms. In our computational experiments, we showed that the FSMI algorithm achieved more than three orders of magnitude computational savings when compared to the original algorithm for computing Shannon mutual information described in [12], while maintaining higher accuracy. We showed that the Approx-FSMI runs 7 times faster than FSMI with negligible precision loss. We also showed that the Approx-FSMI algorithm has the same asymptotic computational complexity when compared to the Approx-CSQMI algorithm, and that the Approx-FSMI algorithm requires a smaller number of multiplications, when compared to the Approx-CSQMI algorithm. We observed in our computational experiments that the Approx-FSMI algorithm runs twice faster than the Approx-CSQMI algorithm.

REFERENCES

[1] B. Yamauchi, "A frontier-based approach for autonomous exploration," in *Computational Intelligence in Robotics and Automation, 1997. CIRA'97., Proceedings., 1997 IEEE International Symposium on*. IEEE, 1997, pp. 146–151.

[2] W. Burgard, M. Moors, C. Stachniss, and F. E. Schneider, "Coordinated multi-robot exploration," *IEEE Transactions on robotics*, vol. 21, no. 3, pp. 376–386, 2005.

[3] H. H. González-Banos and J.-C. Latombe, "Navigation strategies for exploring indoor environments," *The International Journal of Robotics Research*, vol. 21, no. 10-11, pp. 829–848, 2002.

[4] D. Holz, N. Basilico, F. Amigoni, S. Behnke, *et al.*, "A comparative evaluation of exploration strategies and heuristics to improve them." in *ECMR*, 2011, pp. 25–30.

[5] S. Shen, N. Michael, and V. Kumar, "Stochastic differential equation-based expl oration algorithm for autonomous indoor 3d exploration with a micro-aerial vehicle," *The International Journal of Robotics Research*, vol. 31, no. 12, pp. 1431–1444, 2012.

[6] A. Elfes, "Robot navigation: Integrating perception, environmental constraints and task execution within a probabilistic framework," in *Reasoning with Uncertainty in Robotics*. Springer, 1996, pp. 91–130.

[7] A. R. Cassandra, L. P. Kaelbling, and J. A. Kurien, "Acting under uncertainty: Discrete bayesian models for mobile-robot navigation," in *Proceedings of IEEE/RSJ International Conference on Intelligent Robots and Systems. IROS'96*, vol. 2. IEEE, 1996, pp. 963–972.

[8] S. J. Moorehead, R. Simmons, and W. L. Whittaker, "Autonomous exploration using multiple sources of information," in *Robotics and Automation, 2001. Proceedings 2001 ICRA. IEEE International Conference on*, vol. 3. IEEE, 2001, pp. 3098–3103.

[9] F. Bourgault, A. A. Makarenko, S. B. Williams, B. Grocholsky, and H. F. Durrant-Whyte, "Information based adaptive robotic exploration," in *Intelligent Robots and Systems, 2002. IEEE/RSJ International Conference on*, vol. 1. IEEE, 2002, pp. 540–545.

[10] D. Holz, N. Basilico, F. Amigoni, and S. Behnke, "Evaluating the efficiency of frontier-based exploration strategies," in *ISR 2010 (41st International Symposium on Robotics) and ROBOTIK 2010 (6th German Conference on Robotics)*. VDE, 2010, pp. 1–8.

[11] A. Mobarhani, S. Nazari, A. H. Tamjidi, and H. D. Taghirad, "Histogram based frontier exploration," in *2011 IEEE/RSJ International Conference on Intelligent Robots and Systems*. IEEE, 2011, pp. 1128–1133.

[12] B. J. Julian, S. Karaman, and D. Rus, "On mutual information-based control of range sensing robots for mapping applications," *The International Journal of Robotics Research*, vol. 33, no. 10, pp. 1375–1392, 2014.

[13] E. Nelson and N. Michael, "Information-theoretic occupancy grid compression for high-speed information-based exploration," in *Intelligent Robots and Systems (IROS), 2015 IEEE/RSJ International Conference on*. IEEE, 2015, pp. 4976–4982.

[14] B. Charrow, S. Liu, V. Kumar, and N. Michael, "Information-theoretic mapping using cauchy-schwarz quadratic mutual information," in *Proceedings - IEEE International Conference on Robotics and Automation*, 2015.

[15] B. Charrow, G. Kahn, S. Patil, S. Liu, K. Goldberg, P. Abbeel, N. Michael, and V. Kumar, "Information-theoretic planning with trajectory optimization for dense 3d mapping." in *Robotics: Science and Systems*, vol. 6, 2015.

[16] W. Tabib, M. Corah, N. Michael, and R. Whittaker, "Computationally efficient information-theoretic exploration of pits and caves," in *2016 IEEE/RSJ International Conference on Intelligent Robots and Systems (IROS)*. IEEE, 2016.

[17] S. Thrun, W. Burgard, and D. Fox, *Probabilistic robotics*. MIT press, 2005.

[18] J. M. Rabaey, A. P. Chandrakasan, and B. Nikolic, *Digital integrated circuits*. Prentice hall Englewood Cliffs, 2002, vol. 2.

[19] T. H. Cormen, C. E. Leiserson, R. L. Rivest, and C. Stein, *Introduction to algorithms*. MIT press, 2009.

[20] S. Karaman and E. Frazzoli, "Sampling-based algorithms for optimal motion planning," *The international journal of robotics research*, vol. 30, no. 7, pp. 846–894, 2011.

[21] J. Reeds and L. Shepp, "Optimal paths for a car that goes both forwards and backwards," *Pacific journal of mathematics*, vol. 145, no. 2, pp. 367–393, 1990.